# Closed-Form CRLBs for the SNR Estimates from Turbo-Coded PAM- and Rectangular-QAM-Modulated Signals


Achref Methenni and Sofiène Affes
INRS-EMT, 800, De La Gauchetière West, Suite 6900, Montreal, QC, H5A 1K6, Canada.
Emails: {methenni, affes}@emt.inrs.ca



***Abstract*—In this paper, we consider the problem of signal-to-noise ratio (SNR) estimation from turbo-coded (TC) PAM and rectangular-QAM (RQAM) modulated signals over flat-fading channels. We derive for the first time closed-form expressions for the Cramér-Rao lower bounds (CRLBs) of the SNR estimates. We exploit the structure of the binary-reflected-Gray-code (BRGC) for bits-to-symbols mapping, so that the likelihood function (LF) becomes factorized into a sum of two simple terms. This factorization allows the linearization of the log-likelihood function (LLF), which allowed us to carry the derivation of the Fisher Information Matrix (FIM) elements *analytically*, and derive the code aided (CA) SNR CRLB in closed-form (CF). These new CF expressions corroborate the CA bounds established previously in the particular case of square-QAM constellations. They finally tackle the new problem never addressed until now of CA SNR estimation from PAM/RQAM signals. In the low-to-medium SNR level, the new CRLBs for the CA estimates of the SNR range between their respective CRLBs in the non-data-aided (NDA) and data-aided (DA) scenarios, thereby highlighting and quantifying the advantage of CA estimation against the NDA. In high SNR, they coincide with the DA CRLB. These bounds also confirm the increase in estimation accuracy achievable by decreasing the coding rate.**



***Index terms*—** Signal-to-noise ratio (SNR), Cramér-Rao lower bound (CRLB), Parameter estimation, Turbo codes, Turbo processing, extrinsic information, Code-assisted (CA), Gray mapping, PAM, Rectangular QAM.


## I. INTRODUCTION

Signal-to-noise ratio (SNR) is a parameter of major significance in many communications areas, and particularly in wireless systems. It is in fact a key measure of the channel quality [1] and it is therefore needed (and almost omnipresent) in multiple applications such as equalization [2], link adaptation, adaptive modulation, and power control [3], among many others. On another hand, turbo codes [4,5] (TC) have an ongoing attraction to the research community, thanks to their impressive capacity to achieve high data rate, very close to the Shannon capacity limit. In this context, the SNR further plays a more crucial role.

The SNR is generally unavailable at either side of the communication channel. That is why an estimation process is needed to acquire (approximately) these parameters [6]. Depending on the receivers' knowledge of the transmitted symbols, there are mainly two categories of estimators. The first class is that of non-data-aided (NDA) estimators which do not assume any *a priori* knowledge of the data and, hence, consider the received symbols independent and equally likely. The major asset of this approach is that it ensures high throughput since it requires no additional overhead and operates solely on the desired data sequence to be transmitted. However, it exhibits poor performance in the low-to-average SNR regime[1]. The second class of DA estimators exploits the fact that the pilot symbol sequence to deal with is known both to transmitter and the receiver. Although this method enhances the estimation accuracy since the symbols are known, it has the inconvenience of reducing the throughput of the system.

To circumvent the drawbacks on both ends, and in light of the use of powerful error correcting codes like turbo codes, a code-aided (CA) approach has emerged as a solution that combines both benefits of NDA and DA by offering a better estimation performance quality (compared to NDA), yet without the least overhead penalty on the overall throughput (compared to DA). This technique takes advantage of the decoding process and exploits the information it provides about symbols' probabilities to construct more accurate estimates of the desired parameters. Furthermore, using the turbo principle, CA estimators can be designed in an iterative fashion leading to far better performance. This process is called *turbo processing*. For instance, it has been shown in [6] that the SNR estimation performance can be substantially enhanced by exploiting some priors[2] that are delivered during the decoding process of the transmitted bits.

Consequently, these estimators are reversely influenced by the performance of the decoding process: at one decoding iteration, an erroneous decoding of the received sequence will lead to a less accurate estimate. This interdependence between estimation and decoding in the CA scenarios renders the problem of finding the ultimate performance limit of such schemes more challenging. One such limit that addresses the best achievable estimation performance is the well-known fundamental CRLB [7] that sets the minimum achievable variance for any unbiased estimator. The derivation of closed-form expressions fors the CRLBs in typical wireless communications scenarios is a difficult task, and sometimes an impossible one, because of the complex structure of the likelihood function, particularly for high-order modulations. This is why these bounds are usually evaluated empirically in most cases.


Work supported by the Discovery Grants and the CREATE PERSWADE <www.create-perswade.ca> Programs of NSERC and a Discovery Accelerator Supplement Award from NSERC.


[1]At high SNR, the estimator acts like data-aided (DA), as if it knew the symbols.

[2]In CA schemes, the transmitted symbols are also completely unknown. Yet, substantial information about the latter can be acquired during iterative decoding and then exploited in estimation as *a priori* knowledge.


978-1-5090-1328-9/16/$31.00 ©2016 IEEE

The first SNR CRLBs in closed-form expressions were derived in the DA scenario in [8] for different modulations types and orders. In the same work, they were likewise obtained in the NDA case only for BPSK and QPSK modulations. This seminal work was much later followed by [9] that ultimately found, almost a decade later, a solution for the enduring predicament of the CRLBs' generalization in closed form to arbitrary high-order square-QAM modulations despite the increasingly intricate form of the likelihood function. It was just recently that a closed-form CRLB for SNR estimation from turbo-coded square-QAM modulated signals was found [10].

Incited by all of the above-mentioned facts, we derive for the very first time analytical expressions for the CRLBs of the SNR estimates from turbo-coded general PAM and RQAM signals. These new bounds corroborate their empirical counterparts. They also show the advantage of CA over NDA and DA in terms of performance accuracy and signalling overhead, respectively, and the potential estimation gains achievable by decreasing the coding rate.

The remainder of this paper is organized as follows: In section II, we introduce the system model. In section III, we develop new expressions for the BRGC symbols' *a priori* probabilities (APPs) in the cases of general PAM and RQAM constellations in terms of their conveyed bits' log-likelihood ratios (LLRs). In section IV, we derive the LLFs of both modulation types. In section V, we ultimately derive novel closed-form expressions for the considered CRLBs and constellations. In section VI, we assess these new bounds by simulations. Finally, we draw out some concluding remarks in section VII.

## II. System Model

Consider a wireless communication system where a binary sequence is grouped into blocks of equal length $N_b$ bits per block. These data bits pass through a turbo encoder which consists of two identical recursive and systematic convolutional codes (RSCs) with different generator polynomials $[g1,\ g2]$, concatenated in parallel via an interleaver of size $N_b$. The overall coding rate $R_c$ is fixed by the puncturer[3]. Each block of $N_c$ coded bits is fed to an outer interleaver, and then labelled onto a Gray-coded constellation. The obtained symbols sequence travels over the wireless flat-fading channel. At the receiver side, the signal passes through a matched filter $p(t)$, which is supposed to verify the first Nyquist criterion. Throughout this paper, we assume *perfect timing synchronization*. In the presence of phase and CFO distortions, the observed samples are modeled as follows:

$$y_k \ = \ S\, x_k e^{j(2\pi k\nu+\phi)} + w_k, \quad k = k_0, k_0+1, \cdots, k_0+K-1, \tag{1}$$

where, at the sampling index $k$ ($k_0$ refering to the instant of the first sample), $x_k$ is the $k^{th}$ coded symbol transmitted over the wireless channel and $y_k$ is its corresponding received sample. The channel is assumed to be slowly time-varying over the entire observation window of length $K$, and therefore has constant but unknown gain, $S$, and phase offset $\phi$. The parameter $\nu$ stands for the normalized CFO, as mentioned before. The coded sequence $x_k$ is drawn from any $M$-ary PAM or $M_1$x$M_2$-RQAM Gray-labeled constellation. Without loss of generality, we further assume the total energy of the transmitted sequence $x_k$ to be unitary, i.e., $\mathrm{E}\{|x_k|^2\} = 1$. The additional term $w_k$ stems from the noise components modeled by a sequence of zero-mean complex circular Gaussian random variables with independent real and imaginary parts, each of variance $\sigma^2$ (i.e., total noise power is $N_0 = 2\sigma^2$).

The true SNR, $\rho$, we wish to estimate is defined as:

$$\rho \ = \ \frac{\mathrm{E}\{S^2|x_k|^2\}}{2\sigma^2} \ = \ \frac{S^2}{2\sigma^2}. \tag{2}$$

From (2), there are two unknown parameters which are involved in the derivation of the SNR CRLB, namely $S$ and $\sigma^2$. Therefore, it is mathematically more convenient to gather them into a single parameter vector $\boldsymbol{\delta} = [S \quad \sigma^2]$. Depending on the SNR scale (i.e., the SNR in the *decibels* [dB] or *linear* scale), we define the following transformations:

$$g(\boldsymbol{\delta}) = \begin{cases} 10\log_{10}\left(S^2/2\sigma^2\right) & \text{(in [dB] scale)}, \\ S^2/2\sigma^2 & \text{(in linear scale)}. \end{cases} \tag{3}$$

For mathematical convenience, we gather as well all the recorded data samples in a single vector:

$$\boldsymbol{y} = [y_{k_0}, y_{k_0+1}, \cdots, y_{k_0+K-1}]^T. \tag{4}$$

Now suppose that we are able to produce an unbiased estimate, $\hat{\boldsymbol{\delta}}$, of the parameter vector $\boldsymbol{\delta}$, from the received vector $\boldsymbol{y}$. Then, the CRLB is a practical lower bound [7] that verifies[4] the inequality $\mathrm{E}\left\{[\hat{\boldsymbol{\delta}}-\boldsymbol{\delta}][\hat{\boldsymbol{\delta}}-\boldsymbol{\delta})]^T\right\} \succeq \mathrm{CRLB}(\boldsymbol{\delta})$ and is given by:

$$\mathrm{CRLB}(\boldsymbol{\delta}) = \boldsymbol{I}^{-1}(\boldsymbol{\delta}), \tag{5}$$

where $\boldsymbol{I}(\boldsymbol{\delta})$ is the FIM whose entries are expressed by:

$$[\boldsymbol{I}(\boldsymbol{\delta})]_{i,l} = -\mathrm{E}\left\{\frac{\partial^2 L(\boldsymbol{y};\boldsymbol{\delta})}{\partial\delta_i\partial\delta_l}\right\} \qquad i,l = 1,2. \tag{6}$$

In (6), $\{\delta_i\}_{i=1,2,3,4}$ are the elements of the unknown parameter vector $\boldsymbol{\delta}$ and $L(\boldsymbol{y};\boldsymbol{\delta}) \triangleq \ln\left(p[\boldsymbol{y};\boldsymbol{\delta}]\right)$ is the LLF $\big(p[\boldsymbol{y};\boldsymbol{\delta}]$ is the pdf of $\boldsymbol{y}$ parameterized by $\boldsymbol{\delta}\big)$. As shown in [7], the CRLB for the parameter transformation in (3) is given by:

$$\mathrm{CRLB}(\rho) = \frac{\partial g(\boldsymbol{\delta})}{\partial\boldsymbol{\delta}}\boldsymbol{I}^{-1}(\boldsymbol{\delta})\frac{\partial g(\boldsymbol{\delta})}{\partial\boldsymbol{\delta}}^T, \tag{7}$$

The derivative, $\partial g(\boldsymbol{\delta})/\partial\boldsymbol{\delta}$, is given by:

$$\frac{\partial g(\boldsymbol{\delta})}{\partial\boldsymbol{\delta}} = \begin{cases} \begin{bmatrix}\frac{20}{\ln(10)S} & \frac{-10}{\ln(10)\sigma^2}\end{bmatrix} & \text{(in [dB] scale)}, \\ \begin{bmatrix}\frac{S}{\sigma^2} & -\frac{S^2}{2\sigma^4}\end{bmatrix} & \text{(in linear scale)}. \end{cases} \tag{8}$$

As seen from (6), the first challenging step in deriving the targeted bounds is to find an explicit expression for the LLF or equivalently the pdf $p[\boldsymbol{y};\boldsymbol{\delta}]$. To that end, the APPs, $P[x_k = c_m]$, of the transmitted symbols involved in (1) must be found.

## III. Factorization of $p\big[y_k;\boldsymbol{\delta}\big]$

Throughout this paper, we assume that the constellation is Gray labeled. Each point of the alphabet, $\{c_m\}_{m=1}^M$, is mapped onto a unique sequence of $\log_2(M)$ bits denoted here as $\bar{b}_1^m\bar{b}_2^m\cdots\bar{b}_l^m\cdots\bar{b}_{\log_2(M)}^m$. For the sake of clarity, this mapping will be denoted as follows:

$$c_m \longleftrightarrow \bar{b}_1^m\bar{b}_2^m\cdots\bar{b}_l^m\cdots\bar{b}_{\log_2(M)}^m. \tag{9}$$

[3]This rate can be adjusted by changing the turbo code's puncturing matrix.

[4]For square matrices $\boldsymbol{A}$ and $\boldsymbol{B}$, $\boldsymbol{A}\succeq\boldsymbol{B}$ means $\boldsymbol{A}-\boldsymbol{B}$ is positive semi-definite.

The same notation is used to refer to the $k^{th}$ bit sequence, $b_1^k b_2^k \cdots b_l^k \cdots b_{\log_2(M)}^k$, that is conveyed during the transmission of the $k^{th}$ symbol $x_k$, i.e., $x_k \longleftrightarrow b_1^k b_2^k \cdots b_l^k \cdots b_{\log_2(M)}^k$. Due to the large-size interleaver, it is reasonable to assume that the coded bits are statistically independent. This is a standard assumption in CA estimation practices (see [5,11]). Therefore, the *a priori* probability of each transmitted symbol, $x_k$, factorizes into the elementary probabilities of its conveyed bits:

$$P[x_k = c_m] = P\left[\bigcap_{l=1}^{\log_2(M)} b_l^k = \bar{b}_l^m\right] = \prod_{l=1}^{\log_2(M)} P\left[b_l^k = \bar{b}_l^m\right]. \tag{10}$$

Let us also define the LLR of the $l^{th}$ coded bit, $b_l^k$, conveyed by the transmission of the symbol, $x_k$, as the quantity $L_l(k) \triangleq \ln\left(P[b_l^k = 1]/P[b_l^k = 0]\right)$.Using this definition and the fact that $P[b_l^k = 0] + P[b_l^k = 1] = 1$, it can be easily shown that:

$$P[b_l^k = \bar{b}_l^m] = \frac{1}{2\cosh\left(\frac{L_l(k)}{2}\right)} e^{(\bar{b}_l^m - 1)\frac{L_l(k)}{2}}, \tag{11}$$

in which $\bar{b}_l^m$ is either 0 or 1 depending on which of the symbols $c_m$ is transmitted, at time instant $k$, and of course on the Gray mapping that is associated to the constellation in (9). Therefore, injecting (11) in (10) and recalling that $\log_2(M) = p$ for PAM constellations, the symbols' APPs develop into:

$$P[x_k = c_m] = \underbrace{\left(\prod_{l=1}^{p} \frac{1}{2\cosh\left(\frac{L_l(k)}{2}\right)}\right)}_{\beta_{1\to p}^k} \prod_{l=1}^{p} e^{(\bar{b}_l^m - 1)\frac{L_l(k)}{2}}. \tag{12}$$

Recall from (6) that an explicit expression for the global LLF, $L(\boldsymbol{y};\boldsymbol{\delta}) \triangleq \ln\left(p[\boldsymbol{y};\boldsymbol{\delta}]\right)$, must be found before being able to derive the analytical CRLBs. Actually, since the coded bits are assumed to be statistically independent (due to the large-size interleaver), the transmitted symbols (which are simply some *soft* representations for different blocks of these bits) are also independent, thereby leading to:

$$p[\boldsymbol{y};\boldsymbol{\delta}] = \prod_{k=k_0}^{k_0+K-1} p[y_k;\boldsymbol{\delta}]. \tag{13}$$

Consequently, the global LLF breaks down to the sum of the elementary LLFs (pertaining to each received sample), i.e., $L(\boldsymbol{y};\boldsymbol{\delta}) = \sum_{k=k_0}^{k_0+K-1} \ln\left(p[y_k;\boldsymbol{\delta}]\right)$. Then, it can be seen from (1) that the pdf of each received sample, $y_k$, parameterized by the unknown parameter vector, $\boldsymbol{\delta}$, is given by:

$$\begin{aligned} p\left[y_k;\boldsymbol{\delta}\right] &= \sum_{c_m\in\mathcal{C}_p} P\left[x_k = c_m\right]\; p\left[y_k;\boldsymbol{\delta}|x_k = c_m\right] \\ &= \frac{1}{2\pi\sigma^2}\sum_{c_m\in\mathcal{C}_p} P\left[x_k = c_m\right] \exp\left\{\frac{|y_k - S_{\phi,\nu}c_m|^2}{2\sigma^2}\right\}, \end{aligned} \tag{14}$$

in which we use the shorthand notation $S_{\phi,\nu} \triangleq S e^{j(2\pi k\nu+\phi)}$. Then, denoting the inphase (I) and quadrature (Q) components of the received sample, respectively, as $I_k \triangleq \Re\{y_k\}$ and $Q_k \triangleq \Im\{y_k\}$, it can be shown that the pdf in (14) can be rewritten as follows:

$$p[y_k;\boldsymbol{\delta}] = \frac{1}{2\pi\sigma^2}\exp\left\{-\frac{I_k^2 + Q_k^2}{2\sigma^2}\right\} D_{\boldsymbol{\delta}}(k), \tag{15}$$

| | | | | | | | | |
|---|---|---|---|---|---|---|---|---|
| **p=1** | 0 | 1 | | | | | | |
| **p=2** | 1 | 0 | 0 | 1 | | | | |
| | 0 | 0 | 1 | 1 | | | | |
| **p=3** | 1 | 0 | 0 | 1 | 1 | 0 | 0 | 1 |
| | 1 | 1 | 0 | 0 | 0 | 0 | 1 | 1 |
| | 0 | 0 | 0 | 0 | 1 | 1 | 1 | 1 |

Fig. 1. Gray labeling for PAM constellations, for different modulation orders.

in which the term $D_{\boldsymbol{\delta}}(k)$ is defined as:

$$\begin{aligned} D_{\boldsymbol{\delta}}(k) \;\triangleq\; &\sum_{c_m\in\mathcal{C}_p} P[x_k = c_m]\exp\left\{-\frac{S^2\,|c_m|^2}{2\sigma^2}\right\} \\ &\times \exp\left\{\frac{\Re\left\{c_m y_k^* S_{\phi,\nu}\right\}}{\sigma^2}\right\}. \end{aligned} \tag{16}$$

Next, we describe a simple recursive procedure that permits the construction of arbitrary Gray-coded PAM and RQAM constellations.

### A. $P[x_k = c_m]$ *derivation for PAM constellations:*

A general PAM constellation, when $M = 2^p$ for any $p \geq 1$, is defined by:

$$\mathcal{C} = \{\pm(2i-1)d_p\}, \quad i = 1, 2, ..., 2^{p-1}, \tag{17}$$

where $2d_p$ is the intersymbol distance. Since the PAM constellation energy is supposed to be normalized to one, from which the expression of $d_p$ is obtained as follows:

$$d_p = \sqrt{\frac{2^{p-1}}{\sum_{m=1}^{2^{p-1}}(2m-1)^2}}. \tag{18}$$

In Fig. 1 we provide the Gray labeling (BRGC) construction of PAM constellations. It is easy to verify that this recursive procedure leads to a Gray-labelled constellation.
Another important property that can be drawn from this construction due to the symmetry in "*Step 2*" is that each two symbols $\tilde{c}_m$ and $-\tilde{c}_m$ share the same $p-1$ most significant bits (MSBs), $\bar{b}_1^m\bar{b}_2^m\bar{b}_3^m...\bar{b}_{p-2}^m\bar{b}_{p-1}^m$, for any given symbol $\tilde{c}_m$ from the right half-space of the $2^p$-PAM constellation. Thus, if we consider these $p-1$ MSBs and define:

$$\mu_k(c_m) \triangleq \prod_{l=1}^{p-1} e^{(2\bar{b}_m^l - 1)\frac{L_l(k)}{2}}, \qquad \forall c_m \in \mathcal{C}, \tag{19}$$

it follows that:

$$\mu_k(\tilde{c}_m) = \mu_k(-\tilde{c}_m), \qquad \forall \tilde{c}_m \in \tilde{\mathcal{C}}. \tag{20}$$

Then, we have [5]

$$P[x_k = \pm\tilde{c}_m] = \beta_k\ \mu_k(\tilde{c}_m)\ e^{\pm\frac{L_p(k)}{2}} \tag{21}$$

### B. *LLF for PAM signals:*

The term $D_\delta(k)$ defined in (16) needs to be further developed in order to derive the analytical expressions for the

[5]We will omit the index $1 \to p$, to alleviate the notations, unless necessary.

considered CRLBs. When $M=2^p$ for any $p\geq 1$ (i.e., general PAM constellations), we have $\mathcal{C}=\{\pm(2i-1)d_p\}_{i=1,2,...,2^{p-1}}$, where $2d_p$ is the intersymbol distance. Now by denoting $\tilde{\mathcal{C}}=\{+(2i-1)d_p\}_{i=1}^{2^{p-1}}$ the subset of the alphabet that consists of the points which lie in the right sub-plane of the constellation, one can write $\mathcal{C}=\tilde{\mathcal{C}}\cup(-\tilde{\mathcal{C}})$. Therefore, replacing the probabilities $P[x_k=\pm\tilde{c}_m]$ by their expressions in (21), injecting these APPs in (16) and using the identity $e^x+e^{-x}=2\cosh(x)$, it can be shown that:

$$D_\delta(k)=2\beta_k\sum_{\tilde{c}_m\in\tilde{\mathcal{C}}}\exp\left\{-\frac{S^2|\tilde{c}_m|^2}{2\sigma^2}\right\}\mu_k(\tilde{c}_m) \times\cosh\left(\frac{\Re\left\{\tilde{c}_m\ y_k^* S e^{j\phi}\right\}}{\sigma^2}+\frac{L_p(k)}{2}\right). \tag{22}$$

It can also be shown that $\mu_k(\tilde{c}_m)$ can expressed as a recursive function of $i$ as follows:

$$\mu_k(\tilde{c}_m)=\theta_{k,p}(i). \tag{23}$$

The initialization for $p=1$ (i.e., the basic BPSK constellation) is given by $\theta_{k,1}(.)=1$, since $\mu_k(\tilde{c}_m)=1\ \forall\ \tilde{c}_m\in\tilde{\mathcal{C}}_1$. Now, the term $D_\delta(k)$ can be ultimately written as follows:

$$D_\delta(k)=2\beta_k\ F_p(u_k), \tag{24}$$

where $F_p(.)$ is given by:

$$F_p(x)=\sum_{i=1}^{2^{p-1}}\theta_{k,p}(i)\exp\left\{-\frac{S^2(2i-1)^2d_p^2}{2\sigma^2}\right\} \times\cosh\left(\frac{(2i-1)d_pSx}{\sigma^2}+\frac{L_p(k)}{2}\right). \tag{25}$$

where $u_k$ defined as $u_k\triangleq\Re\left\{y_k^*e^{j(\phi+2\pi k\nu)}\right\}$ can be expressed as:

$$u_k=I_k\cos(2\pi k\nu+\phi)+Q_k\sin(2\pi k\nu+\phi). \tag{26}$$

If we also define $v_k\triangleq\Im\left\{y_k^*e^{j(\phi+2\pi k\nu)}\right\}$, which can be developed into:

$$v_k=I_k\sin(2\pi k\nu+\phi)-Q_k\cos(2\pi k\nu+\phi), \tag{27}$$

using the fact that $I_k^2+Q_k^2=u_k^2+v_k^2$, it can be shown that $p[y_k;\boldsymbol{\delta}]$ itself is factorized as follows: Finally, the LF of $y_k$ is given by:

$$p[y_k;\boldsymbol{\delta}]=\overbrace{\frac{1}{\sqrt{2\pi\sigma^2}}\exp\left\{-\frac{v_k^2}{2\sigma^2}\right\}}^{p[v_k;\boldsymbol{\delta}]}\underbrace{\frac{2\beta_k}{\sqrt{2\pi\sigma^2}}\exp\left\{-\frac{u_k^2}{2\sigma^2}\right\}F_p(u_k)}_{p[u_k;\boldsymbol{\delta}]}. \tag{28}$$

Moreover, we have $p[y_k^*e^{j(2\pi k\nu+\phi)};\boldsymbol{\delta}]=p[u_k,v_k;\boldsymbol{\delta}]$ since $u_k$ and $v_k$ are indeed the real and imaginary parts of $y_k^*e^{j(2\pi k\nu+\phi)}$. Furthermore, since the synchronization parameters $\phi$ and $\nu$ are assumed to be deterministic, we readily have $p[y_k^*e^{j(2\pi k\nu+\phi)};\boldsymbol{\delta}]=p[y_k^*;\boldsymbol{\delta}]=p[y_k;\boldsymbol{\delta}]$. This leads to $p[u_k,v_k;\boldsymbol{\delta}]=p[y_k;\boldsymbol{\delta}]$ which is combined with (28) to yield:

$$p[u_k,v_k;\boldsymbol{\delta}]\quad=\quad p[u_k;\boldsymbol{\delta}]p[v_k;\boldsymbol{\delta}], \tag{29}$$

meaning that $u_k$ and $v_k$ are indeed two independent random variables (RVs) which are distributed according to (28).

### C. $P[x_k=c_m]$ *derivation for RQAM constellations:*

A RQAM constellation can be defined, when $M=2^{p_1+p_2}$ for any $p_1,p_2\geq 1$ and $i=1,2,...,2^{p_1-1};n=i=1,2,...,2^{p_2-1}$, as:

$$\mathcal{C}=\{\pm(2i-1)d_{p_1+p_2}\pm j(2n-1)d_{p_1+p_2}\}, \tag{30}$$

where $2d_{p_1+p_2}$ is the intersymbol distance[6]. Once again, we suppose the RQAM constellation energy to be unitary, from which the expression of $d_{p_1+p_2}$ is obtained as follows:

$$\frac{1}{d_{p_1+p_2}^2}=\sum_{i=1}^{2^{p_1-1}}\frac{(2i-1)^2}{2^{p_1-1}}+\sum_{n=1}^{2^{p_2-1}}\frac{(2n-1)^2}{2^{p_2-1}}. \tag{31}$$

The Gray labeling for a $2^{p_1+p_2}$-QAM constellation is then constructed as the *cartesian product* of two Gray-labelled (using the Gray mapping scheme of PAM excplicited in the previous section) PAM constellations: $2^{p_1}$-PAM$\times 2^{p_2}$-PAM , one for the real part of the QAM constellation (the first $p_1$ MSBs $\bar{b}_1^m\bar{b}_2^m\cdots\bar{b}_{p_1}^m$) and one for the imaginary part (the remaining $p_2$ bits $\bar{b}_{p_1+1}^m\bar{b}_{p_1+2}^m\cdots\bar{b}_{p_1+p_2}^m$).

It is straightforward to show that this construction yields, from its use of two Gray-labeled PAM constellations, a Gray-labeled RQAM constellation. Since the coded bits are assumed independent, the real and imaginary parts of a rectangular $2^{p_1+p_2}$-QAM constellation symbol are also independent:

$$\begin{aligned}P[x_k=\tilde{c}_m]&=P[(\Re\{x_k\},\Im\{x_k\})=(\Re\{\tilde{c}_m\},\Im\{\tilde{c}_m\})] \\ &=P[\Re\{x_k\}=\Re\{\tilde{c}_m\}]\times P[\Im\{x_k\}=\Im\{\tilde{c}_m\}].\end{aligned} \tag{32}$$

Treating the real and imaginary parts of the symbol $\tilde{c}_m$ like two PAM constellations and defining as in (19):

$$\mu_k(\Re\{c_m\})\triangleq\prod_{l=1}^{p_1-1}e^{(2\bar{b}_m^l-1)\frac{L_l(k)}{2}},\quad\forall c_m\in\mathcal{C}, \tag{33}$$

$$\mu_k(\Im\{c_m\})\triangleq\prod_{l=p_1+1}^{p_1+p_2-1}e^{(2\bar{b}_m^l-1)\frac{L_l(k)}{2}},\quad\forall c_m\in\mathcal{C}, \tag{34}$$

we can deduce, like in the PAM case, that:

$$\mu_k(\Re\{\tilde{c}_m\})=\mu_k(-\Re\{\tilde{c}_m\}),\quad\forall\tilde{c}_m\in\tilde{\mathcal{C}}, \tag{35}$$

$$\mu_k(\Im\{\tilde{c}_m\})=\mu_k(-\Im\{\tilde{c}_m\}),\quad\forall\tilde{c}_m\in\tilde{\mathcal{C}}. \tag{36}$$

Then, we have:

$$P[\Re\{x_k\}=\pm\Re\{\tilde{c}_m\}]=\beta_{k,1}\ \mu_k(\Re\{\tilde{c}_m\})\ e^{\pm\frac{L_{p_1}(k)}{2}}, \tag{37}$$

$$P[\Im\{x_k\}=\pm\Im\{\tilde{c}_m\}]=\beta_{k,2}\ \mu_k(\Im\{\tilde{c}_m\})\ e^{\pm\frac{L_{p_1+p_2}(k)}{2}}. \tag{38}$$

The above equations form the complete set of APPs for each symbol $x_k$.

### D. *LLF for RQAM signals:*

In the following, we will factorize the pdf $p[y_k;\boldsymbol{\delta}]$ in the R-QAM case. Furthermore, since the synchronization parameters $\phi$ and $\nu$ are assumed to be deterministic, we readily have $p[y_k;\boldsymbol{\delta}]=p[y_k^*;\boldsymbol{\delta}]=p[y_k^*e^{j(2\pi k\nu+\phi)};\boldsymbol{\delta}]$. On the other hand, since:

$$y_k=S\ x_ke^{j(2\pi k\nu+\phi)}+w_k, \tag{39}$$

[6]The intersymbol distance for RQAM is defined by two integers, one for each dimension.

we can establish that:

$$y_k^* e^{j(2\pi k\nu+\phi)} = S\ x_k^* + \tilde{w}_k, \tag{40}$$

where $\tilde{w}_k \triangleq w_k^* e^{j(2\pi k\nu+\phi)}$. We can now underline the following properties:

- Since the coded bits are assumed to be independent, the real and imaginary parts of $x_k$ are independent. Consequently, the real and imaginary parts of $S\ x_k^*$ are independent.
- Since $w_k$ is a *circular* additive white gaussian noise (CAWGN), $\tilde{w}_k$ is a complex CAWGN with *independent* real and imaginary parts.
- The noise samples $w_k$ and the transmitted symbols $x_k$ are independent. Hence, so are $\tilde{w}_k$ and $S\ x_k^*$.

Owing to these properties, we can deduce that $\Re\{y_k^* e^{j(2\pi k\nu+\phi)}\}$ and $\Im\{y_k^* e^{j(2\pi k\nu+\phi)}\}$ are independent. And these quantities are nothing but $u_k$ and $v_k$ defined in the previous subsection. Hence, we have:

$$p[y_k;\boldsymbol{\delta}] = p[u_k;\boldsymbol{\delta}]p[v_k;\boldsymbol{\delta}], \tag{41}$$

where, in this case, $u_k$ and $v_k$, now have the following distributions:

$$p\big[u_k;\boldsymbol{\delta}\big] = \frac{2\beta_{k,1}}{\sqrt{2\pi\sigma^2}}\exp\left\{-\frac{u_k^2}{2\sigma^2}\right\}F_{p_1,\boldsymbol{\delta}}(u_k), \tag{42}$$

$$p\big[v_k;\boldsymbol{\delta}\big] = \frac{2\beta_{k,2}}{\sqrt{2\pi\sigma^2}}\exp\left\{-\frac{v_k^2}{2\sigma^2}\right\}F_{p_2,\boldsymbol{\delta}}(v_k), \tag{43}$$

with

$$\beta_{k,1} = \beta_{1\to p_1}^k, \quad \text{and} \quad \beta_{k,2} = \beta_{p_1+1\to p_1+p_2}^k, \tag{44}$$

where, in (42) and (43), we resort to the same function $F_{p,\boldsymbol{\delta}}(x)$ used in the case of PAM constellations, yet with sums over $p_1$ terms for $u_k$ and $p_2$ terms for $v_k$ in the RQAM case. Also the additive term inside the cosh changes from $\frac{L_p(k)}{2}$ in the PAM case to $\frac{L_{p_1}(k)}{2}$ (last bit of the first group of bits) and $\frac{-L_{p_1+p_2}(k)}{2}$ (last bit of the second group of bits) for $u_k$ and $v_k$, respectively, in the RQAM case[7].

The above factorization of $p[y_k;\boldsymbol{\delta}]$ is actually the cornerstone result behind enabling for the very first time the derivation in the next section of the analytical expressions for the considered stochastic CRLBs over RQAM transmissions.

## IV. Derivation of the CA CRLBs

Our starting point is the expression of the FIM elements defined in (6). And we are now ready to find the explicit expression for the global LLF, $L(\boldsymbol{y};\delta) \triangleq \ln(p[\boldsymbol{y};\boldsymbol{\delta}])$. In fact, by injecting (28) in (13), it follows that:

$$L(\boldsymbol{y};\boldsymbol{\delta}) = -K\ln\left(2\pi\sigma^2\right) + \sum_{k=k_0}^{k_0+K-1}\ln\left(D_{\boldsymbol{\delta}}(k)\right) - \frac{I_k^2+Q_k^2}{2\sigma^2}. \tag{45}$$

### A. PAM constellations

For PAM constellations, after recalling that $D_{\boldsymbol{\delta}}(k) = 2\beta_k F_{p,\boldsymbol{\delta}}(u_k)$ and dropping all the terms which are irrelevant when deriving with respect to $S$, the LLF defined above becomes:

$$L(\boldsymbol{y};\boldsymbol{\delta}) = \sum_{k=k_0}^{k_0+K-1}\ln\big(F_{p,\boldsymbol{\delta}}(u_k)\big). \tag{46}$$

The FIM term pertaining to the channel gain $S$ is given by:

$$\mathrm{E}_{\boldsymbol{y}}\left\{\frac{\partial^2\ln(p[\boldsymbol{y};\boldsymbol{\delta}])}{\partial S^2}\right\} = \sum_{k=k_0}^{k_0+K-1}\mathrm{E}\left\{\frac{\partial^2\ln(F_p(u_k))}{\partial S^2}\right\}. \tag{47}$$

We will only develop the main results here since their derivations are very similar to those of the previous subsection. In fact, we can prove through the same approach as before that the first diagonal element of $\boldsymbol{I}(\boldsymbol{\delta})$ is given by:

$$\mathrm{E}_{\boldsymbol{y}}\left\{\frac{\partial^2\ln(p[\boldsymbol{y};\boldsymbol{\delta}])}{\partial S^2}\right\} = -\frac{1}{\sigma^2}\sum_{k=k_0}^{k_0+K-1}\Delta_{k,p}, \tag{48}$$

where $\Delta_{k,p} \triangleq 2\beta_{k,p}d_p^2\Lambda_{k,p}(\rho)$ and the function $\Lambda_{k,p}(.)$ is defined as:

$$\Lambda_{k,p}(\rho) \triangleq \frac{1}{\sqrt{2\pi}}\int_{-\infty}^{+\infty}\frac{\lambda_{k,p}^2(\rho,t)}{\delta_{k,p}(\rho,t)}\ e^{-\frac{t^2}{2}}dt. \tag{49}$$

where, by using $\omega_{k,p_1}^{(l)}(i) \triangleq (2i-1)^l\theta_{k,p_1}(i)\ e^{-(2i-1)^2 d_{p_1+p_2}^2\rho}$, the functions $\delta_{k,p_1}(.,.)$ and $\lambda_{k,p_1}(.,.)$ are given by:

$$\delta_{k,p_1}(\rho,t) = \sum_{i=1}^{2^{p_1-1}}\omega_{k,p_1}^{(0)}(i)\cosh(t_{i,p_1}), \tag{50}$$

$$\lambda_{k,p_1}(\rho,t) = T_{p_1,\sqrt{2\rho}}^{(1)}(t), \tag{51}$$

where

$$T_{p,\alpha}^{(l)}(t) = \sum_{i=1}^{2^{p-1}}\omega_{k,p}^{(l)}(i)\Big[t\sinh(t_{i,p}) - d_p(2i-1)\alpha\cosh(t_{i,p})\Big], \tag{52}$$

and $t_{i,p} = \sqrt{2\rho}(2i-1)d_p t + \frac{L_p(k)}{2}$. Equivalent algebraic manipulations, which are omitted here for the sake of conciseness, lead to the following analytical expressions for the second FIM's diagonal element:

$$\mathrm{E}_{\boldsymbol{y}}\left\{\frac{\partial^2\ln(p[\boldsymbol{y};\boldsymbol{\delta}])}{\partial{\sigma^2}^2}\right\} = \frac{1}{\sigma^4}\sum_{k=k_0}^{k_0+K-1}\upsilon_{k,p}, \tag{53}$$

where $\upsilon_{k,p}$ is given by:

$$\upsilon_{k,p} = c_{4,p}^{(k)}\rho^2 + 2\rho\left(c_{2,p}^{(k)} - 2\beta_{k,p}d_p^2\Upsilon_{k,p}(\rho)\right) - c_{0,p}^{(k)}. \tag{54}$$

The coefficients $c_{l,p}^{(k)}$ are given by:

$$c_{l,p}^{(k)} = 2\beta_{k,p}d_p^l\cosh\left(L_p(k)/2\right)\sum_{i=1}^{2^{p-1}}\theta_{k,p}(i)(2i-1)^l, \tag{55}$$

and the function $\Upsilon_{k,p}(.)$ is defined as:

$$\Upsilon_{k,p}(\rho) \triangleq \frac{1}{\sqrt{2\pi}}\int_{-\infty}^{+\infty}\frac{\gamma_{k,p}^2(\rho,t)}{\delta_{k,p}(\rho,t)}\ e^{-\frac{t^2}{2}}dt, \tag{56}$$

where $\gamma_{k,p}(.,.)$ is given by:

$$\gamma_{k,p}(\rho,t) = T_{p,\sqrt{\frac{\rho}{2}}}^{(2)}(t_{i,p}). \tag{57}$$

[7]The minus one "$-1$" in the $\frac{-L_{p_1+p_2}(k)}{2}$ is due to the minus one "$-1$" in $v_k = -S\ \Im\{x_k\} + \Im\{\tilde{w}_k\}$.

Equivalent derivations also yield the following expression for the off-diagonal element of $\boldsymbol{I}(\boldsymbol{\delta})$:

$$\mathrm{E}_{\boldsymbol{y}}\left\{\frac{\partial^2 \ln(p[\boldsymbol{y};\boldsymbol{\delta}])}{\partial\sigma^2\partial S}\right\} = -\frac{S}{\sigma^4}\sum_{k=k_0}^{k_0+K-1}\varepsilon_{k,p}, \tag{58}$$

in which $\varepsilon_{k,p} \triangleq c_{2,p}^{(k)} - 2d_p^2\, \beta_{k,p}\, \xi_{k,p}(\rho)$ with the function $\xi_{k,p}(.)$ being defined as:

$$\xi_{k,p}(\rho) \triangleq \frac{1}{\sqrt{2\pi}}\int_{-\infty}^{+\infty}\frac{\gamma_p(\rho,t)\lambda_p(\rho,t)}{\delta_p(\rho,t)}\ e^{-\frac{t^2}{2}}dt. \tag{59}$$

Therefore, the global FIM decomposes into the sum of elementary FIMs:

$$\boldsymbol{I}_{p,\boldsymbol{\delta}}(\rho) = \sum_{k=k_0}^{k_0+K-1}\boldsymbol{I}_{k,p,\boldsymbol{\delta}}(\rho), \tag{60}$$

where $\{\boldsymbol{I}_{k,p,\boldsymbol{\delta}}(\rho)\}_{k=k_0}^{k_0+K-1}$ is the FIM pertaining to the estimation of the SNR from the received sample $y_k$ alone:

$$\boldsymbol{I}_{k,p,\boldsymbol{\delta}}(\rho) = \frac{1}{\sigma^4}\begin{pmatrix}\sigma^2\Delta_{k,p} & S\varepsilon_{k,p}\\ S\varepsilon_{k,p} & -\upsilon_{k,p}\end{pmatrix}. \tag{61}$$

We should first mention that the FIM elements do not depend here on the shape of the transmit pulse. So as long as the pulse shape verifies the first Nyquist criterion and is unitary, it will not appear in the CRLB expression. After some algebraic manipulations, it can be shown that the overall CRLB for CA SNR estimates (in *linear scale*) of PAM signals is given by:

$$\mathrm{CRLB}(\rho) = f_\rho(\bar{\boldsymbol{\upsilon}}_p, \bar{\varepsilon}_p, \bar{\boldsymbol{\Delta}}_p), \tag{62}$$

where

$$f_\rho(x,y,z) \triangleq \frac{2\rho x - \rho^2(4y+z)}{xz - 2\rho y^2}, \tag{63}$$

and the generic term $\bar{\boldsymbol{\upsilon}}$ is defined as:

$$\bar{\boldsymbol{\upsilon}} \triangleq \sum_{k=0}^{K-1}\upsilon_k. \tag{64}$$

where $k_0$ was set to zero since it does not affect the estimation performance of the SNR.

### B. RQAM constellations

In the RQAM case, the LLF defined in (45) reduces after dropping all terms irrelevant to the derivations related to the parameters $S$ and $\phi$ to:

$$L(\boldsymbol{y};\boldsymbol{\delta}) = \sum_{k=k_0}^{k_0+K-1}\ln\left(F_{p_1}(u_k)\right) + \ln\left(F_{p_2}(v_k)\right), \tag{65}$$

The FIM elements for the case of RQAM are derived in a similar fashion to that of PAM constellations. Due to space limitations, we will provide here the final expression of the CA SNR CRLB in this case.

In order to explicitly express the CA CRLBs, one must use the corresponding FIM, $\boldsymbol{I}(\boldsymbol{\delta})$ which is valid for both *linear* and *decibels* [dB] scales. In particular, if one is using the *linear* scale, then the corresponding CA CRLB CA SNR estimates (in *linear scale*) of RQAM signals is given by:

$$\mathrm{CRLB}(\rho) = f_\rho(\bar{\boldsymbol{\upsilon}}_{p_1} + \bar{\boldsymbol{\upsilon}}_{p_2} + K, \bar{\varepsilon}_{p_1} + \bar{\varepsilon}_{p_2}, \bar{\boldsymbol{\Delta}}_{p_1} + \bar{\boldsymbol{\Delta}}_{p_2}). \tag{66}$$

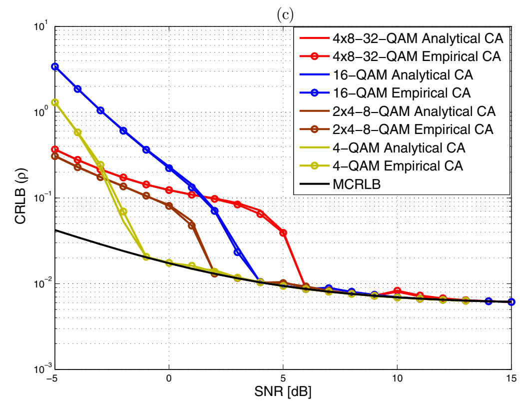


Fig. 2. Analytical and empirical CA CRLBs of the SNR for different RQAM modulations and coding rate $R_c = 1/3$.

The CRLB for CA SNR estimates in the [dB] scale is directly deduced from the CA CRLB in the *linear* scale, given by (66), as follows:

$$\underbrace{\mathrm{CRLB}(\rho)}_{\text{in [dB] scale}}\ [\mathrm{dB}^2] = \frac{100}{\ln(10)^2\rho^2}\underbrace{\mathrm{CRLB}(\rho)}_{\text{in linear scale}}. \tag{67}$$

## V. Simulation Results

In this section, we illustrate by simulations the new closed-form CRLBs of the different parameters with various modulation orders and different coding rates using $K = 3270$ coded symbols each time. The turbo code consists of two identical RSCs both of nominal rate $R_0 = 1/2$ and of generator polynomials (1,1,0,1) and (1,0,1,1), respectively. The puncturer is configured so as to obtain the desired overall coding rate $R_c$.

The extrinsic information delivered by the turbo decoder is used to evaluate the bit LLRs, $L_l(k)$, which are in turn injected in the CA SNR estimation CRLB expression to evaluate it. In all simulations, we use the *extrinsic* information obtained at the $8^{th}$ turbo iteration(after the decoder reach a steady state and both constituent SISO decoders converge). In all the subsequent simulations, we plot the CRLBs of the SNR CRLBs in [dB$^2$] against the nominal SNR in [dB].

We start by verifying in Fig. 2 that the newly obtained closed-form expressions for the CA CRLBs coincide with their *empirical* counterparts[8]. Indeed, an extremely large number of noisy observations was generated in order to find an empirical value for the expectation involved in the FIM for the considered parameters. In contrast, our new closed-form expressions allow the immediate evaluation of the CRLBs from any turbo-coded PAM and RQAM signals. Furthermore, we observe that in the RQAM case, there is no *strict order* relationship holding over the entire SNR range between the CRLBs and the modulation size (i.e., the former increasing with the latter) in the most general case of RQAM modulations mixing both square and non-square QAM. However, within each of these two sub-classes, such order relationship holds indeed (i.e., 8-QAM<32-QAM and 4-QAM<16-QAM).

We plot in Fig. 3 the CA CRLBs for different PAM modulation orders. As expected, we verify that the CA CRLBs are

[8]The SNR CA CRLBs have never been established before for the case of PAM and general RQAM, neither empirically nor analytically.

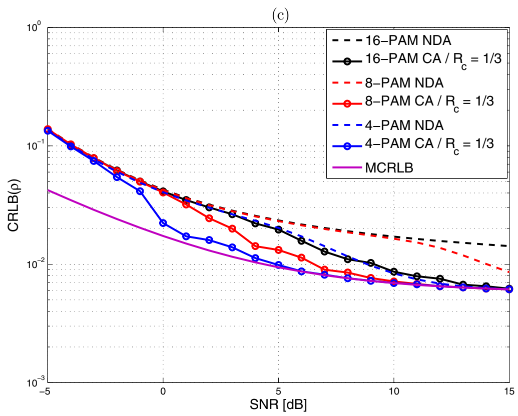


Fig. 3. Analytical CA and NDA CRLBs of the SNR for different PAM modulations and $R_c = 1/3$.

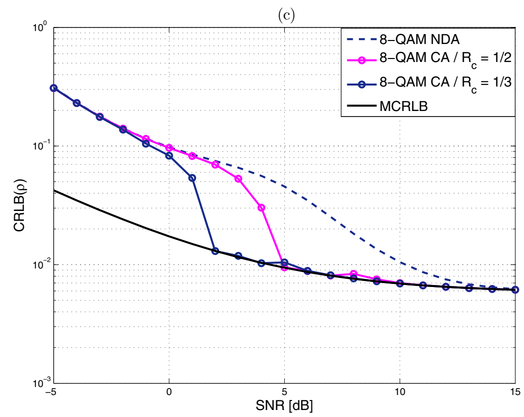


Fig. 4. Analytical CA CRLBs of the SNR and for different coding rates and 2x4-8-QAM modulation.

smaller than the NDA CRLBs derived recently in [12]. This predicted result highlights and quantifies the potential estimation performance gain that could be achieved by leveraging the information about the transmitted bits one could gather during the decoding process. It is in contrast with the traditional NDA scheme where the considered parameters are estimated directly from the output of the matched filter. Even though the CA scheme performs next to the CRLB limit nearly as well as the NDA scheme at low SNR, at the vicinity of -3 dB, it always offers a potential gain (over the latter) that sharply increases with the SNR increasing. For instance, by the SNR value $\rho = 0$ dB, the CA CRLB for 4-PAM signals soon becomes twice smaller than the NDA CRLB. Additionally and most prominently, the CA CRLBs decrease rapidly and reach the modified CRLBs (MCRLBs), the ideal bounds that would be obtained if all the transmitted symbols were perfectly known to the receiver, which are given by:

$$\text{MCRLB} = \frac{100}{K \ln^2(10)} \left(1 + \frac{2}{\rho}\right) \qquad \text{for the SNR.} \tag{68}$$

We also notice that the CA CRLB for the $4$-PAM modulation is distinctly lower than the CA CRLB for higher orders. In fact, when the order is greater than $4$, all CA CRLBs start to approach each other very fast to the point where we can hardly notice any visible improvement from using higher-order PAM. Similar performance behavior has been previously reported [12] in the case of NDA estimation.

In Fig. 4, we illustrate the effect of the coding rate on the turbo estimation performance by plotting the CRLBs with 2x4-8-QAM modulation and the two coding rates $R_c = 0.3285 \approx \frac{1}{3}$ and $R_c = 0.4892 \approx \frac{1}{2}$. Even though the CA CRLBs corresponding to the two considered rates ultimately coincide at moderate SNR levels, they exhibit a significant gap at lower SNR values. In fact, with smaller coding rates, more redundancy can potentially be provided by the turbo encoder and the bits could then be decoded more accurately. In this case, the *extrinsic* information, which is used to approximate the LLRs, becomes increasingly higher (in absolute value) and CA estimation becomes even closer in CRLB performance to DA estimation.

## VI. Conclusion

In this paper, we established for the first time analytical expressions of the CRLBs for SNR estimation from turbo-coded PAM- and RQAM-modulated signals over *flat-fading* channels. We exploited the structure of Gray-labeled PAM and RQAM constellations enabled us to simplify the LLF and calculate the FIM elements and, hence, the considered CRLBs in closed-form. The new derived bounds coincide with their empirical counterparts. They also range between the NDA and DA CRLBs, thereby highlighting and quantifying the advantage of CA over NDA estimation. At high SNR, the CA CRLBs coincide with the DA bounds thereby implying near-optimal CA estimation performance in that regime.

## References

[1] S. Nanda, K. Balachandran, and S. Kumar, “Adaptation techniques in wireless packet data services,” *IEEE Trans. Commun.* vol. 38, no. 1, pp. 54-64, Jan. 2000.

[2] S. Talakoub and B. Shahrrava, “Turbo equalization with iterative online SNR estimation,” in *Proc. IEEE WCNC*, New Orleans, USA, 2005

[3] K. Balachandran, S. R. Kadaba, and S. Nanda, “Channel quality estimation and rate adaptation for cellular mobile radio,” *IEEE J. Sel. Areas Commun.,* vol. 17, no. 7, pp.1244 -1256, July 1999.

[4] C. Berrou, “The ten-year old turbo codes are entering into service”, *IEEE J. Commun. Mag.*, vol. 41, no. 8, pp. 110-116, Aug. 2003.

[5] C. Berrou and A. Glavieux, “Near optimum error correcting coding and decoding: turbo codes,” *IEEE Trans. Commun.,* vol. 44, no. 10, pp. 1261-1271, Oct. 1996.

[6] M. Bergmann, W. Gappmair, H. Schlemmer, and O. Koudelka, “Code-aware joint estimation of carrier phase and SNR for linear modulation schemes”, in *Proc. 5th Advanced Satellite Multimedia Systems Conference*, Cagliari, Italy, 2010.

[7] S. M. Kay, *Fundamentals of Statistical Signal Processing, Vol. 1: Estimation Theory*, Englewood Cliffs, NJ: Prentice-Hall, 1998.

[8] N. S. Alagha, “Cramér-Rao bounds of SNR estimates for BPSK and QPSK modulated signals,” *IEEE Commun. Lett.,* vol. 5, no. 1, pp. 10-12, Jan. 2001.

[9] F. Bellili , A. Stéphenne, and S. Affes, “Cramér-Rao lower bounds for NDA SNR estimates of square QAM modulated transmissions,” *IEEE Trans. Commun.,* vol. 58, no. 11, pp. 3211-3218, Nov. 2010.

[10] F. Bellili, A. Methenni, and S. Affes , "Closed-form Cramer Rao lower bound for SNR estimation from turbo-coded BPSK-, MSK-, and square-QAM-modulated signals" , *IEEE Trans. Signal Process.,* vol. 62, no. 15, pp. 4018-4033, Aug. 2014.

[11] B. Vucetic, and J. Yuan, *Turbo Codes: Principles and Applications*, Norwell, MA, USA: Kluwer Academic Publishers, 2000.

[12] A. R.-Kebrya, I.-M. Kim, D. I. Kim, F. Chan, and R. Inkol , "Likelihood-based modulation classification for multiple-antenna receiver", *IEEE Trans. Commun.,* vol. 61, no. 9, pp. 3816-3829, Sep. 2013.